IAC-08-C4.4.9

NUMERICAL SIMULATION OF ARGON FLOWS IN CYLINDRICAL SELF-FIELD MPD THRUSTERS

M.Sc. Rouhallah khoshkhoo
Department of Mechanical &Aerospace Engineering, MUT, Tehran, Iran
mahdi.khoshkhoo@gmail.com

Associate professor. Mahmood Adami
Department of Mechanical & Aerospace Engineering, MUT, Tehran, Iran
m_adami_mut@yahoo.com
Dr. Ahmad Sedaghat.
Department of Mechanical Engineering, Isfahan University of Technology, Isfahan, Iran
sadaghat@cc.iut.ac.ir

ABSTRACT

In this paper, the fluid flow in an induced magneto plasma dynamics (MPD) thruster is simulated. The magneto hydrodynamic (MHD) equations are used in conjunction with fully ionized gas. The governing fluid flow Navier-Stokes equations are discretised and solved using a finite difference total variation diminishing (TVD) scheme and the induced magnetic equations are solved using a Successive over Relaxation (SOR) method. Numerical results are presented for argon for a mass flow rate of 2.25 g/s and the electrical currents of 4-7 kA. Also, interaction between fluid flow and magnetic field is parametrically studied. Distribution of density and temperature at thruster exit and also effect of magnetic field on velocity field in the MPD thruster is investigated.

INTRODUCTION

Magneto plasma dynamic (MPD) thruster is one kind of the electromagnetic thrusters that is used for spacecraft engines. These spacecrafts are used for space transportation between planets due to comparable performance with electrical thrusters [1]. These kinds of thrusters have high exhaust particles velocity $(10^4\ m/s)$, much lower thrust density (thrust over exhaust area) compare with other systems; however, having long life, very high flight duration, and high reliability. MPDs require high carrying electrical power and low specific mass [2].

BACKGROUND

Computational researchers have tried to effectively define the physical problem of induced MPD thrusters. Lapoint [3], sleziona and other [4] have developed a numerical model for argon gas using a two dimensional time-dependent model. Lapoint [3] has used the ideal gas state equation for solving ionized MPD equations. He used the method of finite difference for computing the speed, pressure, ion and electron temperature, and flow field properties. He has done his research on different size MPD thrusters.

Sleziona et al. [4] have used a finite volume method for solving Navier- Stokes equations and the Gouse-Seidel method for solving induced electromagnetic equations. They compared their numerical results with experimental data and concluded that the maximum magnetic field is around the cathode section and the magnetic Hall effects are around the anode tip and the cathode root.

Sasaki and Kawaguchi [5] have solved Euler equations for a single fluid using a TVD scheme. They solved electromagnetic equations by the method of SOR. This recent equations are coupled together and show that electromagnetic force is not depended on thruster shape; however because of induced magnetic field, the fluid particles accelerate above cathode surface. Then particle speeds are reduced in down stream of plasma field. The results of this work are compared to results of [5].

Martinez and chanty [6] have solved two dimensional Euler equations in magneto plasma dynamic thrusters with the assumption of single fluid using Newton-Raphson method. The cathode section and magnetic Hall effects are around the anode tip and the cathode root. They observed high acceleration on cathode surface Because of the existence of Lorentz force. Also, the sudden reduction of density at the beginning of insulating surface was observed.

Bery and Roy [7] solved the single fluid two dimensional Navier- Stokes equations for MPD thrusters using a finite-element method. They also analyzed the Hall Effects. They concluded that the electromagnetic force has much more effect on upstream flow with respect to down stream flow. Increase of density causes the increase of radial and axial thrust force and temperature. For this reason, the electrical power loss in electrodes is a big part of total thruster power in agreement with lower prediction of efficiency obtained from practical tests. In constant mass flow rate, increasing of flow cause the increase of exit velocity. The results of current work are also compared to the results of [7].

MPD THRUSTER PERFORMANCE PRINCIPLE

MPD thrusters have a multilayer geometry in witch it is constructed of a central cathode and a cylindrical anode around it. Back surface is made from Brome-Nitride [2]. Gaseous propellants are entered into channel like upstream flow. Gas going through a steady electrical arc (in radial axis r) witch is located between electrodes and so is ionized. If the electrical arc be strong enough, it would produce annular magnetic field (in θ direction). This function is suitable for producing axial and radial forces for propulsion magnitude. This force is obtained from $\vec{F} = \vec{J} \times \vec{B}$ in witch it is called Lorentz force. This force produces the acceleration to forward and axial side is along the central line. A lot of hat plasma exists after the tip of cathode. Expansion of this plasma along axial direction would result in high exit velocity [8]. Figure 1 is showing the performance of MPD thruster.

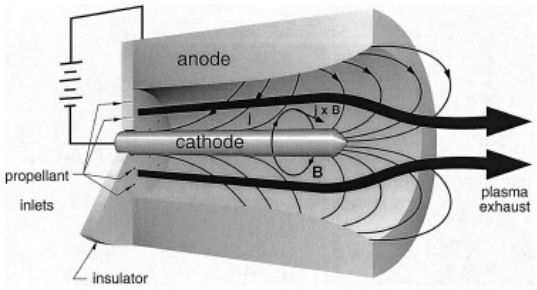

Figure1: A schematic of a magneto plasma dynamic thruster (MPDT)

Total thrust includes electromagnetic and aerodynamic thrust. Electromagnetic thrust is obtained from

$$\tau = \frac{\mu J^2}{4\pi}\left(\ln\left(\frac{r_a}{r_c}\right) + A\right) \quad (1)$$

Increase of electrical current causes the increase of exit velocity. This results in increase of total thrust. This should be noticed that if the mount of electrical current in increases too much, than, the exit velocity and thrust would get to an analogical amount which is not accessible. Therefore, Hegel has developed the following experimental relation for critical electrical current for argon gas,

$$\frac{I^2}{\dot{m}} \approx 2.5\times10^{10}(A^2 kg^{-1} s) \quad (2)$$

Maximum electrical current for analyze is 7kA.

NUMERICAL METHOD

TVD numerical methods are methods in witch total variations of each acceptable physical solution is gradually reduced and diminished. Lax and Vondroff [9] have developed the total variation diminishing concept based on an important property from Cartesian conservation law.

$$u_t + f_x = 0 \quad (3)$$

They showed that total variation of each acceptable physical solution which is represented by following relation is not changed by time increasing,

$$TV = \int \left|\frac{\partial u}{\partial x}\right| dx \quad (4)$$

Total variation is an expanded Cartesian conservation law solution like

$$TV(u) = \sum_i \left|u_{i+1} - u_i\right| \quad (5)$$

If following relation be acceptable gas numerical method it is a TVD method,

$$TV(u^{n+1}) \le TV(u^n) \quad (6)$$

FLUID FLOW EQUATIONS

For better understanding of parameters effects, the non-dimensional form of the governing Navier- Stokes equations are used in Cartesian system as follow:

$$\frac{\partial U}{\partial t} + \frac{\partial F(U)}{\partial x} + \frac{\partial G(U)}{\partial y} + H(U) = S \quad (7)$$

S is the source part. U is a vector of conservation variables

$$U = [\rho \quad \rho u \quad \rho v \quad e \quad B]^T \quad (8)$$

u and v are Cartesian velocities, ρ is density, e is total energy per unit of volume, and pressure P is given by:

$$P = (\gamma - 1)[e - \frac{1}{2}\rho(u^2 + v^2)] \quad (9)$$

γ is specific heat ratios.

H, G and F fluxes can be divided into two parts. Sign I is for inviscid and V is for viscous parts,

$$\begin{aligned} F &= F^I + F^V \\ G &= G^I + G^V \\ H &= H^I + H^V \end{aligned} \quad (10)$$

Where,

$$F^V = \begin{bmatrix} 0 \\ -\tau_{xx} \\ -\tau_{xy} \\ -(u\tau_{xx} + v\tau_{xy}) + q_x \end{bmatrix}$$

$$F^I = \begin{bmatrix} \rho u \\ P + \rho u^2 \\ \rho uv \\ eu + pu \end{bmatrix}$$

$$G^V = \begin{bmatrix} 0 \\ -\tau_{xy} \\ -\tau_{yy} \\ -(u\tau_{xy} + v\tau_{yy}) + q_y \end{bmatrix}$$

$$G^I = \begin{bmatrix} \rho v \\ \rho uv \\ P + \rho u^2 \\ ev + pv \end{bmatrix} \qquad (11)$$

$$H^I = \frac{1}{y(i,j)} \begin{bmatrix} \rho v \\ \rho uv \\ \rho v^2 \\ ev + pv \end{bmatrix}$$

$$H^V = \frac{1}{y(i,j)} \begin{bmatrix} 0 \\ -\tau_{xy} + \frac{2}{3}\frac{y(i,j)}{\mathrm{Re}}\frac{\partial}{\partial x}\left(\mu\frac{v}{y(i,j)}\right) \\ -\tau_{yy} + \tau_{\theta\theta} + \frac{2}{3}\frac{\mu}{\mathrm{Re}}\left(\frac{v}{y(i,j)}\right) + \frac{2}{3}\frac{y(i,j)}{\mathrm{Re}}\frac{\partial}{\partial y}\left(\mu\frac{v}{y(i,j)}\right) \\ -u\tau_{xy} - v\tau_{yy} + \frac{2}{3}\frac{\mu}{\mathrm{Re}}\left(\frac{v^2}{y(i,j)}\right) + \frac{2}{3}\frac{y(i,j)}{\mathrm{Re}}\frac{\partial}{\partial y}\left(\mu\frac{v^2}{y(i,j)}\right) - \frac{2}{3}\frac{y(i,j)}{\mathrm{Re}}\frac{\partial}{\partial x}\left(\mu\frac{vu}{y(i,j)}\right) + q_y \end{bmatrix}$$

$$S = \begin{bmatrix} 0 \\ \frac{B_\infty^2}{\rho_\infty U_\infty^2 \mu_\bullet}\frac{\partial B}{\partial x}B \\ \frac{B_\infty^2}{\rho_\infty U_\infty^2 \mu_\bullet}\left(\frac{B^2}{y(i,j)} + \frac{\partial B}{\partial y}B\right) \\ \frac{B_\infty}{\rho_\infty U^3{}_\infty \mu_\bullet}\left(E_y\frac{\partial B}{\partial x} - E_x\left(\frac{B}{y(i,j)} + \frac{\partial B}{\partial y}\right)\right) \end{bmatrix}$$

That U_∞ is the free stream velocity, B is magnetic field, $y(i,j)$ is radial distance from symmetrical axis, B_∞ is free stream magnetic field, superscript * is for dimensional quantities, subscript ∞ is for free stream quantities and $\mu_\bullet$ is Magnetic permeability of free space and tensors of shear stress

$$\tau_{xx} = \frac{\mu}{\mathrm{Re}}\left(\frac{4}{3}\frac{\partial u}{\partial x} - \frac{2}{3}\frac{\partial v}{\partial y}\right)$$
$$\tau_{yy} = \frac{\mu}{\mathrm{Re}}\left(\frac{4}{3}\frac{\partial v}{\partial y} - \frac{2}{3}\frac{\partial u}{\partial x}\right) \qquad (12)$$
$$\tau_{xy} = \frac{\mu}{\mathrm{Re}}\left(\frac{\partial u}{\partial y} + \frac{\partial v}{\partial x}\right)$$

And heat flux vector are as follow

$$q_x = -\frac{\gamma U_\infty^2 \mu}{\mathrm{Pr}\,\mathrm{Re}(\gamma - 1)}\frac{\partial(P/\rho)}{\partial x}$$
$$q_y = -\frac{\gamma\mu}{\mathrm{Pr}\,\mathrm{Re}(\gamma - 1)}\frac{\partial(P/\rho)}{\partial y} \qquad (13)$$

Electrical fields along x and y axes (E_x, E_y) are as follow (L is reference length, in this paper the L equal to electrodes length)

$$E_x = \frac{B_\infty}{\sigma_\infty \mu_\infty L}\frac{1}{\sigma}\left(\frac{\partial B}{\partial y} + \frac{B}{y(i,j)}\right) - U_\infty B_\infty (vB) \qquad (14)$$

$$E_y = -\frac{B_\infty}{\sigma_\infty \mu_\infty L}\frac{1}{\sigma}\left(\frac{\partial B}{\partial x}\right) - U_\infty B_\infty (uB)$$

Induced magnetic equation for non-dimensioning in this method is written as,

$$\frac{\partial B^*}{\partial t^*} - \frac{1}{\sigma\mu_\infty}\left(\frac{\partial^2 B^*}{\partial x^{*2}} + \frac{\partial^2 B^*}{\partial y^{*2}}\right) + \frac{\partial (u^* B^*)}{\partial x^*} + \frac{\partial (v^* B^*)}{\partial y^*} = 0 \qquad (15)$$

In non- dimensioning from,

$$\frac{\partial B}{\partial t} - \frac{1}{\sigma_\infty \mu_\infty U_\infty L}\left(\frac{\partial^2 B}{\partial x^2} + \frac{\partial^2 B}{\partial y^2}\right) + \frac{\partial (uB)}{\partial x} + \frac{\partial (vB)}{\partial y} = 0 \qquad (16)$$

Numerical solution and similarity method for MPD thrusters are shown in figure2.

Few points are to be noticed:

1- In this method the electrical conduct (σ) is assemble to be constant. Plasma electrical conductive coefficient is assumed about 1000 to 10000.in this paper this coefficient is $\sigma_\infty = 10000\ (ohm^{-1}.m^{-1})$
2- In this method the Hall Effect is ignored.
3- In this method, magnetic field variation by time is not considered. Therefore $\frac{\partial B}{\partial t} = 0$ in induced magnetic equation.
4- Plasma gas is assumed fully ionized.
5- Voltage loss, unusual transfer, chemical reaction, and electrodes fatigue are ignored.
6- Plasma equation is assumed to be ideal gas state equation.

Geometric and boundary conditions

In figure 3, combustion boundary condition of MPD thruster is shown. Electrodes are assumed adiabatic. Plasma gas initial temperature is assumed 5000'K. Prandtle number for argon gas is 0.667.

Velocity boundary conditions in MPD thrusters are shown in figure 4. Electromagnetic boundary conditions are shown in figure 5. Field is assumed to be zero for locations far away from electrodes and symmetrical axis.

Size of meshes including the electrodes is 101×154. Meshes geometry is shown in figure 6. Numerical selections of equation by method of TVD are shown in references in Yee [9], Akbari [10], Sedaghat [11, 12].

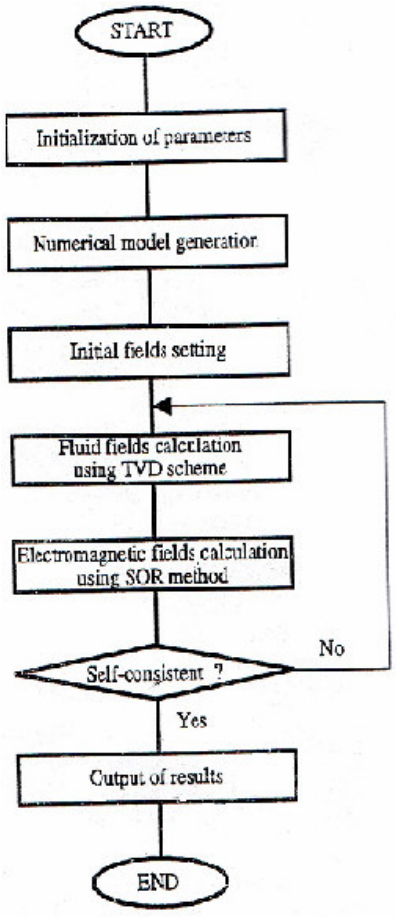

Figure2: The flowchart of numerical algorithm for analyzing MPD thrusters

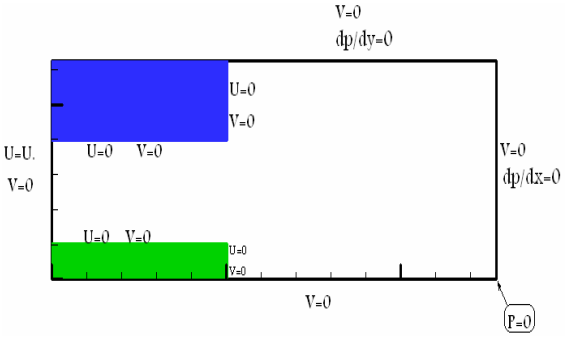

Figure3: The velocity boundary conditions for MPD thruster

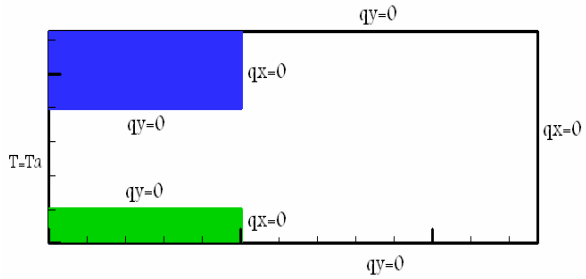

Figure4: The thermal boundary conditions for MPD thruster

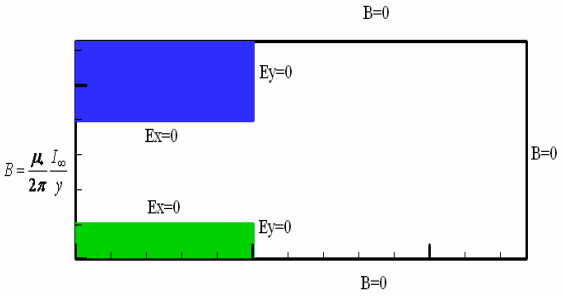

Figure5: The electromagnetic boundary conditions for MPD thruster

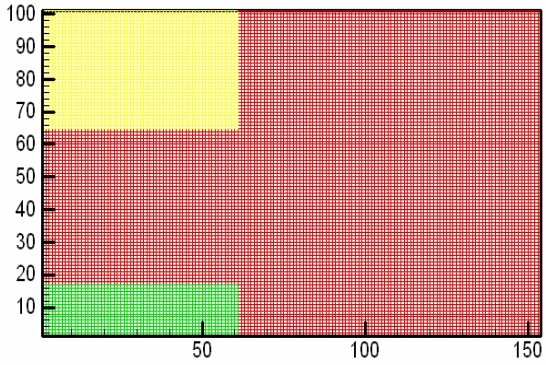

Figure6: Computational domain consist of a mesh of 154×101

DISCUSSION OF RESULTS

At present work, the effort of Lorentz force from magnetic field has been studied over fluid flow. This force causes the increase of plasma fluid velocity. It has more effect on upstream flow than downstream one.

Plasma flow is assumed compressible, independent of time, with an entrance Mach number of 2 and Reynolds number of 270 over the surface of two coaxial circular cylinders. The results are compared with those of references [5, 6, 7, and 13]. The most significant result corresponds to fluid flow density that is suddenly increased at the beginning of entrance and also increased over the cathode surface. These are shown in figure 7. Figure 8 shows the increase of temperature on the cathode surface. Velocity vector field is shown in figure 9. By increasing exit fluid velocity, contours of velocity and electrical current at $I_\infty = 4kA$ are shown in figure 10 and 11, respectively.

Thrust increases by increasing the magnetic field intensity. Figures 12, 13 and 14 show the contours of velocity in electrical currents that induce stronger magnetic field and therefore high thruster exit velocity produces higher thrust force. Figure 15 is reproduced from reference [7]. It shows that the maximum thrust has happened for mass flow of 2.25 g/s in a radius of 3 centimeters. As it is known, the increase of velocity causes the increase of thrust resulting from magnetic field. Variation of velocity, density and temperature at the end of electrodes between the distances of electrodes are shown in figures 16, 17

and 18 respectively. Maximum velocity has occurred at a radius of 3 centimeters which is matched with maximum temperature and minimum of density.

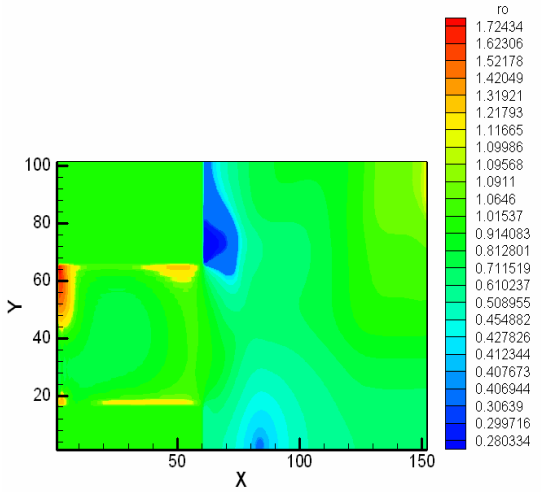

Figure7: Density contour plots for $I_\infty = 4kA$

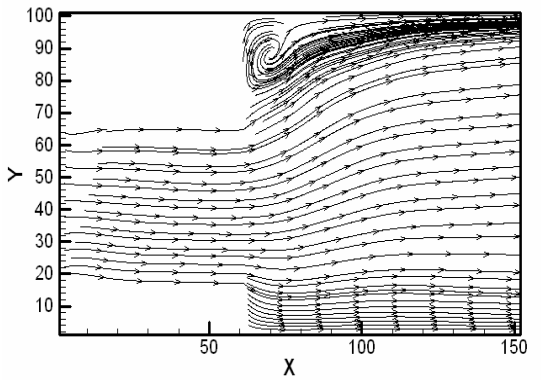

Figure8: Velocity vector field for $I_\infty = 4kA$

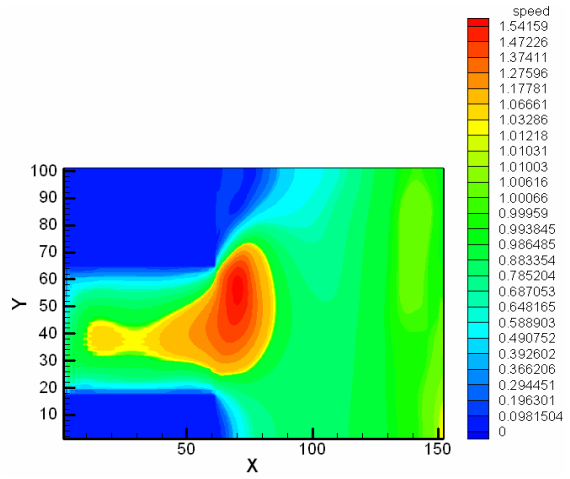

Figure9: Velocity contours for $I_\infty = 4kA$

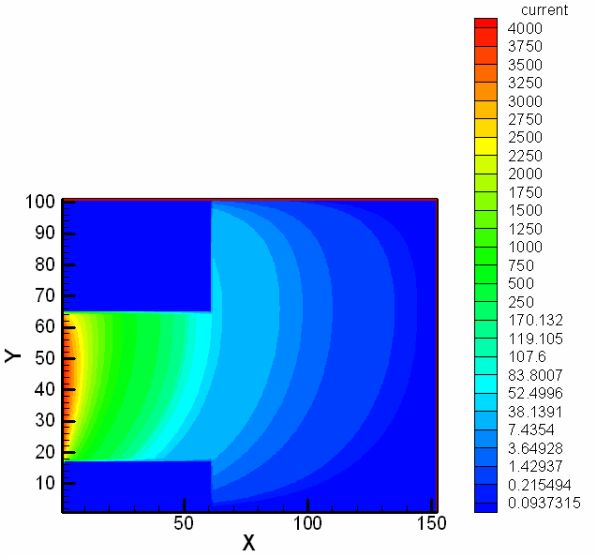

Figure10: Contours of electrical current for $I_\infty = 4kA$

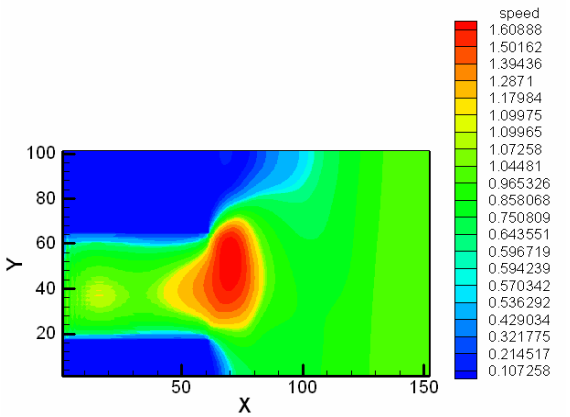

Figure11: Contours of velocity for $I_\infty = 5kA$

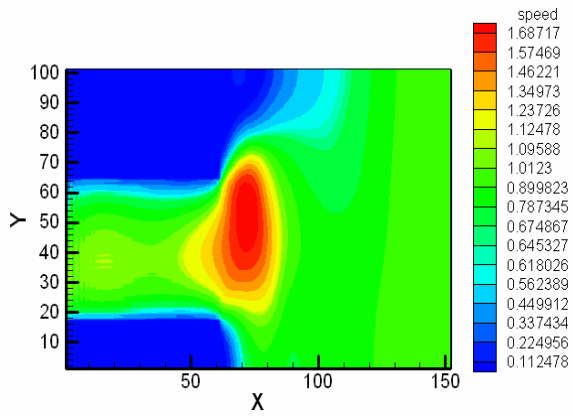

Figure12: Contours of velocity for $I_\infty = 6kA$

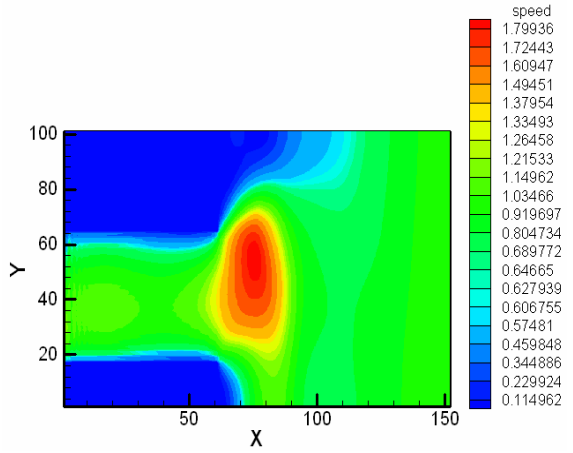

Figure13: Contours of velocity for $I_\infty = 7kA$

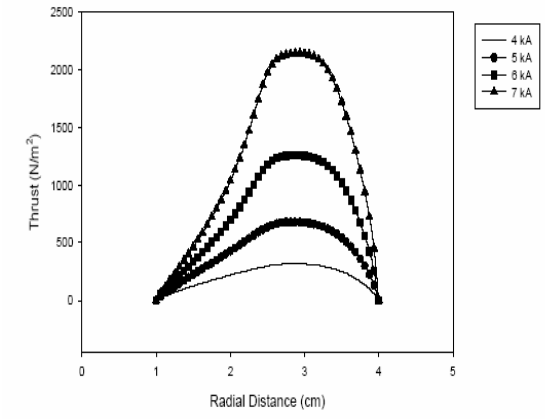

Figure14: Exit thrust vs. current [7]

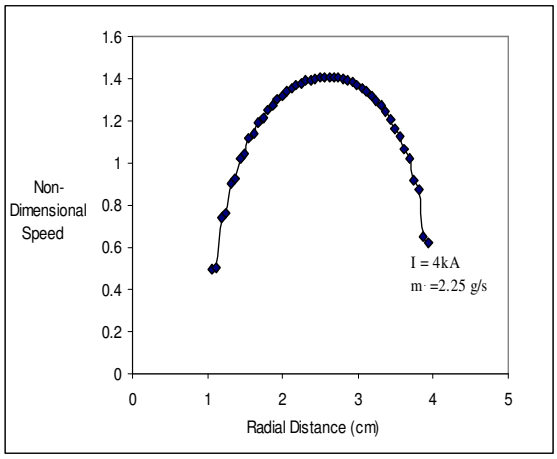

Figure15: The exit velocity versus radial distance

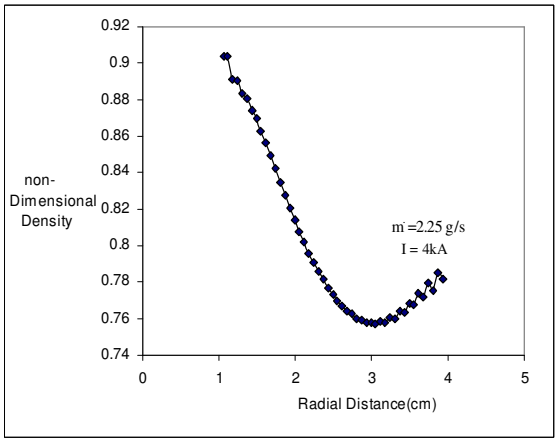

Figure16: Exit density distribution against radial distance

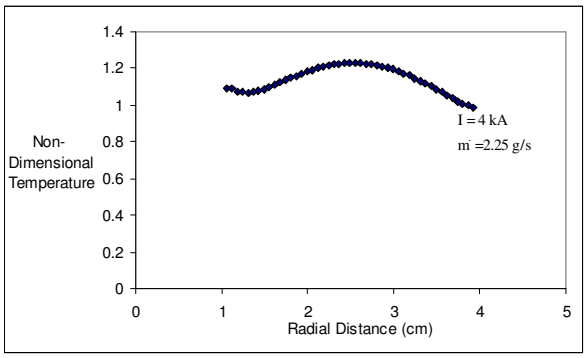

Figure17: Exit temperature distribution versus radial distance

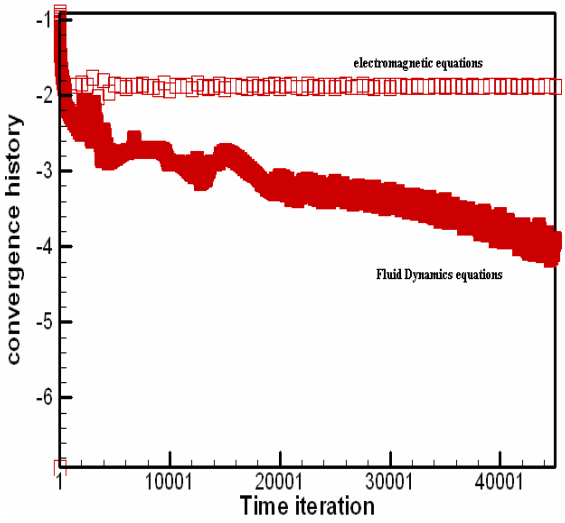

Figure18: Residual of density against time iterations ($I_{\infty} = 4kA$ and $\dot{m} = 2.25 \frac{g}{s}$)

REFERENCES

[1] Michael R., and LaPointe M., High Power MPD Thruster Development at the NASA GLENN RESEARCH CENTER. *NASA/CR_* 2001-211114.

[2] Edgar Jahn., and Choueiri Y., Electric Propulsion. *Encyclopedia of Physical Science and Technology*, Third Edition, Volume. 5.

[3] Lapoite M., Numerical simulation of self-fild mpd thrusters. *AIAA Paper* , No.91-2341, 1991.

[4] Sleziona P.C., and Auweter-Kurtz M., and Schrade H.O., Computation of MPD flows and comparison with experimental results. *Int. Journal for Numerical Methods in Engineering*,Vol.34, 1992, pp.759-771.

[5] Kawaguchi H., and Sasaki K., and Itoh H., Numerical study of the thrust mechanism in a two-dimensional MPD thruster. *Int.J.Applied electromagnetics and Mechanics*,Vol. 6, 1995, pp. 351-365.

[6] Martinez-Sanchez M., and Chanty J.M.G., Two-Dimensional Numerical Simulation Of MPD Flows. *AIAA Paper*, No.87-1090, 1987.

[7] Berry K.J., and Subrata Roy., Finite element based algorithm for self-induced magnetic field applications. *AIAA Paper*, No.2001-0200, 2001.

[8] Lapointe R.Michael., High Power MPD Thruster Performance Measurements. NASA TM -2004-213226, *AIAA*-2004 -3467.

[9] Yee H.C., Implicit Total Variation Diminishing (TVD) schemes for steady-state calculations. *J.Comp. Phys*, V.57, 1985, pp. 327-360.

[10] Akbari S.A., and Sedaghat.A and Azimian R.A., Computational flow Separation Control Using Electromagnetic Fields. *14th Annual (International) Mechanical Engineering Conference*, Isfahan, Iran. May 2006.

[11] Sedaghat A., A Finite Volume TVD Approach to Transonic Flow Computation. *PHD Thesis*, the university of Manchester, 1997.

[12] Sedaghat A., and Azimian A.R., and Akbari S.A., Computational Stall Prevention Using Electromagnetic Fields. *European Conference on Computational Fluid Dynamics*, TUD Delft, the Netherland, 2006.

[13] Kameshwaran Sankaran., Simulation of MPD Flows Using a Flux-Limited Numerical Method for the MHD Equations. *Dissertation of Princeton University*, 2006.